Supporting Information for "Decadal prediction of net primary production in the ocean"

K. M. Krumhardt[1,3], N. S. Lovenduski[2], M. C. Long[3], J. Y. Luo[3,4], K. Lindsay[3], S. Yeager[3], C. Harrison[5]

[1]Environmental Studies Program and Institute of Arctic and Alpine Research, University of Colorado Boulder, Boulder, Colorado, U.S.A.

[2]Department of Atmospheric and Oceanic Sciences and Institute of Arctic and Alpine Research, University of Colorado Boulder, Boulder, Colorado, U.S.A.

[3]Climate and Global Dynamics, National Center for Atmospheric Research, Boulder, Colorado, U.S.A.

[4]NOAA Geophysical Fluid Dynamics Laboratory, Princeton, New Jersey, U.S.A.

[5]Port Isabel Laboratory, University of Texas Rio Grande Valley, U.S.A.

Contents of this file

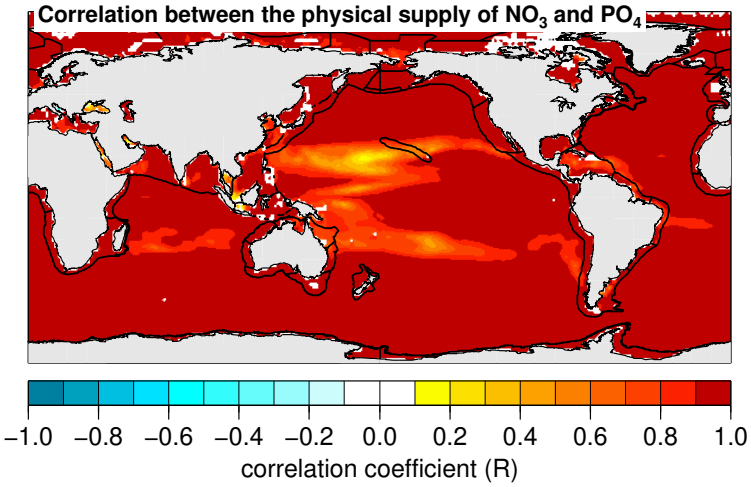

Figure S1. The correlation coefficient between the physical supply of PO_4 and NO_3 over the FOSI reconstruction.

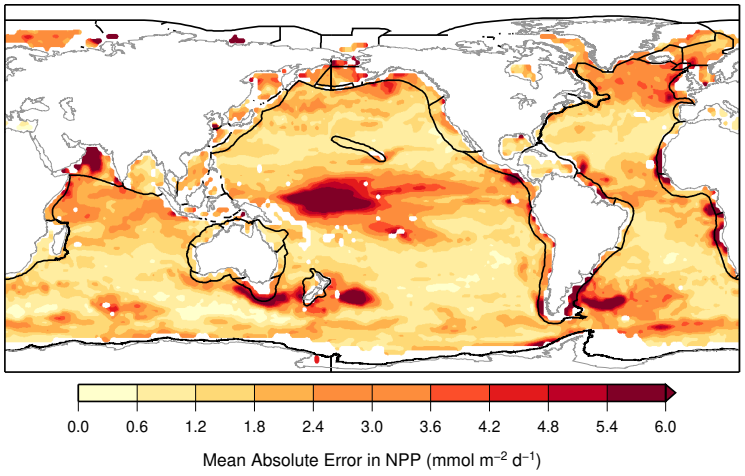

Figure S2. Mean absolute error in the CESM-FOSI reconstruction of NPP and satellite-derived NPP.

Table S1. Anomaly correlation coefficients (ACC) or potential predictability of NPP in the world's Large Marine Ecosystems (LMEs) using the CESM-DPLE forecasts. ACCs in bold are significantly higher than a persistence forecast at the 95% level.

	Potential Predictability (ACC)				
LME	**LY1**	**LY2**	**LY3**	**LY4**	**LY5**
East Bering Sea	0.38	0.31	**0.32**	**0.16**	**0.27**
Gulf of Alaska	**0.52**	**0.29**	0.15	0.02	0.07
California Current	**0.72**	0.32	-0.08	-0.16	-0.02
Gulf of California	**0.84**	0.23	-0.18	-0.26	-0.09
Gulf of Mexico	0.61	0.55	0.41	0.45	0.45
SE US Continental Shelf	**0.81**	0.57	0.14	0.25	0.37
NE US Continental Shelf	0.73	0.50	0.22	0.11	-0.02
Scotian Shelf	0.76	**0.63**	0.41	0.38	0.41
Newfoundland-Labrador Shelf	0.49	0.24	-0.09	-0.17	-0.08
Insular Pacific-Hawiian	**0.77**	**0.59**	**0.50**	0.09	-0.01
Pacific Central-American	0.45	0.53	0.07	-0.17	-0.03
Caribbean Sea	0.64	**0.45**	0.29	0.26	0.17
Humboldt Current	0.47	**0.37**	**0.17**	**0.15**	0.22
Patagonian Shelf	**0.51**	0.34	0.24	**0.20**	0.10
South Brazil Shelf	0.74	0.61	0.47	**0.36**	**0.29**
East Brazil Shelf	0.72	0.56	0.39	0.32	0.33
North Brazil Shelf	0.50	0.31	0.17	0.11	0.13
Canada E. Arctic-W. Greenland	0.43	0.48	**0.44**	**0.38**	**0.21**
Greenland Sea	0.59	0.53	0.42	0.33	0.33
Barents Sea	0.45	0.33	0.26	0.15	0.10
Norwegian Sea	0.11	0.29	0.13	0.15	0.01
North Sea	**0.52**	**0.38**	0.36	0.06	0.09
Celtic-Biscay Shelf	0.19	0.11	-0.02	0.04	-0.17
Iberian Coastal	0.23	0.12	-0.05	-0.05	0.00
Mediterranean	**0.36**	**0.50**	**0.48**	0.36	0.38
Canary Current	0.48	**0.38**	0.19	-0.13	0.14
Guinea Current	0.43	0.35	0.23	0.25	0.17
Benguela Current	0.28	-0.54	-0.52	-0.37	-0.37
Agulhas Current	**0.71**	0.28	-0.17	-0.11	-0.12
Somali Coastal Current	0.17	-0.08	-0.22	-0.30	-0.15
Arabian Sea	0.29	0.31	**0.56**	0.27	0.20
Bay of Bengal	0.49	0.15	-0.29	-0.22	0.08
Gulf of Thailand	0.94	**0.84**	**0.70**	**0.51**	0.34
South China Sea	0.59	0.50	**0.44**	0.20	0.04
Sulu-Celebes Sea	0.47	0.22	-0.06	-0.37	-0.34
Indonesian Sea	0.53	0.27	-0.27	-0.38	-0.10
North Australian Shelf	0.56	0.46	**0.50**	0.30	0.13
NE Australian Shelf	**0.78**	**0.75**	0.33	-0.02	-0.17
E-central Australian Shelf	**0.82**	**0.69**	0.48	0.28	0.13
SE Australian Shelf	**0.40**	**0.28**	0.28	0.29	**0.29**
SW Australian Shelf	**0.71**	0.54	0.44	0.48	**0.59**
W-central Australian Shelf	0.69	0.47	-0.30	-0.35	-0.10
NW Australian Shelf	-0.00	0.15	0.26	0.18	-0.15
New Zealand Shelf	**0.56**	**0.48**	0.15	0.33	**0.33**
East China Sea	0.42	0.36	0.25	0.20	0.11
Yellow Sea	0.59	**0.54**	**0.50**	0.37	0.12
Kuroshio Current	**0.85**	0.68	0.51	0.51	0.25
Sea of Japan/East Sea	0.72	0.55	0.35	0.29	0.25
Oyashio current	0.41	0.24	0.05	0.19	0.16
Sea of Okhotsk	0.43	0.29	0.24	0.13	0.08
West Bering Sea	0.68	0.58	0.33	-0.03	-0.17
N Bering Sea-Chukchi Sea	0.29	0.26	0.21	-0.13	0.05
Beaufort Sea	**0.28**	0.20	0.08	0.22	0.15
East Siberian Sea	-0.10	-0.09	0.22	-0.12	0.02
Laptev Sea	-0.15	-0.05	-0.15	-0.20	-0.06
Kara Sea	0.06	0.11	0.17	0.02	0.08
Iceland Shelf and Sea	0.55	0.54	**0.50**	0.42	**0.26**
Faroe Plateau	0.23	0.20	0.36	0.02	-0.14
Antarctic	0.35	0.55	0.36	0.13	-0.02
Hudson Bay Complex	0.08	0.06	0.03	0.07	0.13
Central Arctic Ocean	0.28	0.31	0.18	**0.30**	0.18
Aleutian Islands	**0.60**	0.47	0.49	**0.40**	0.31
Canadian High Arctic- N Greenland	0.27	0.13	0.20	0.36	0.31

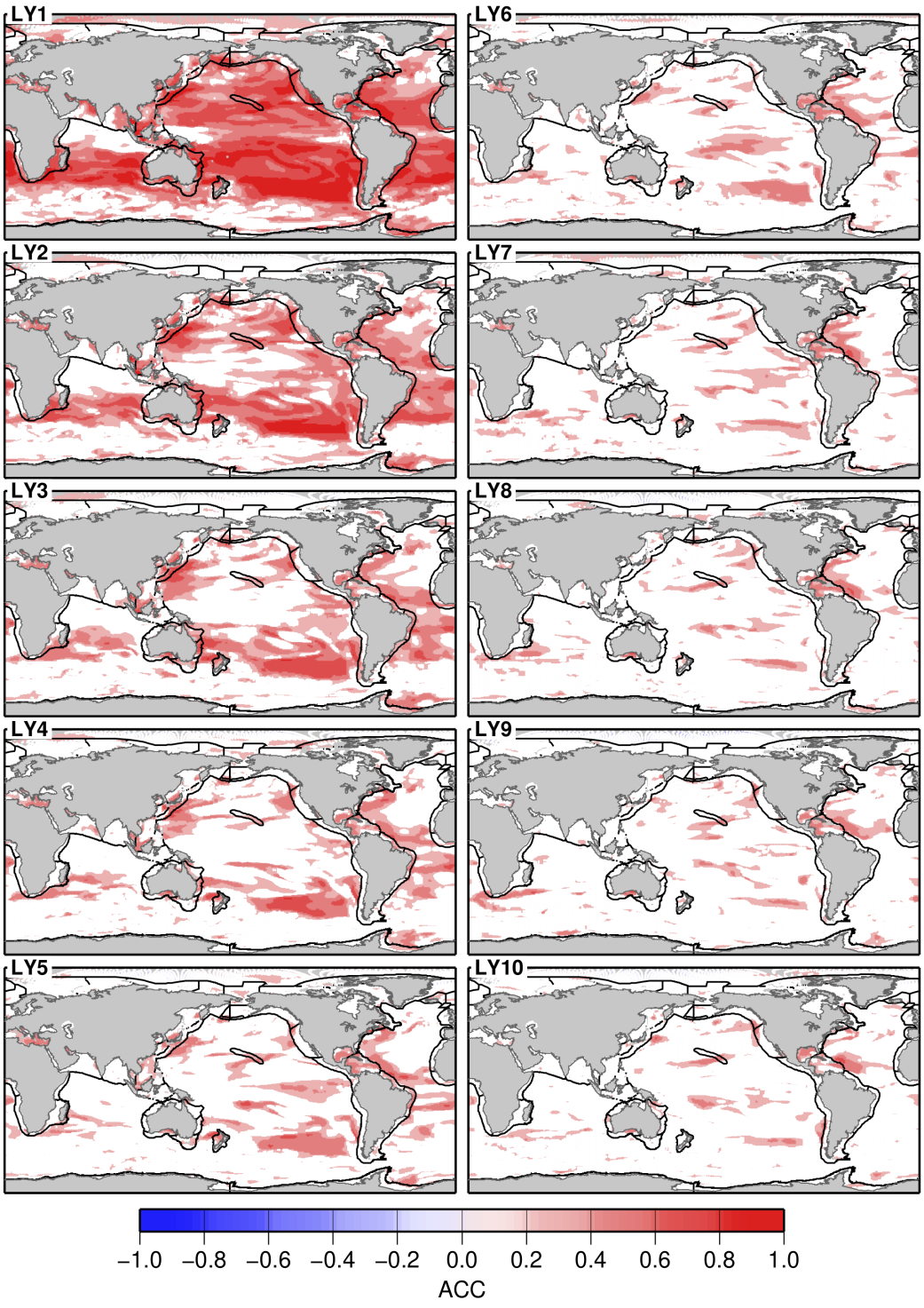

Figure S3. NPP anomaly correlation coefficients (ACC; potential predictability) between the CESM-DPLE NPP forecasts and the CESM-FOSI NPP reconstruction. Only significant correlations are shown; white areas denote non-significant correlations.

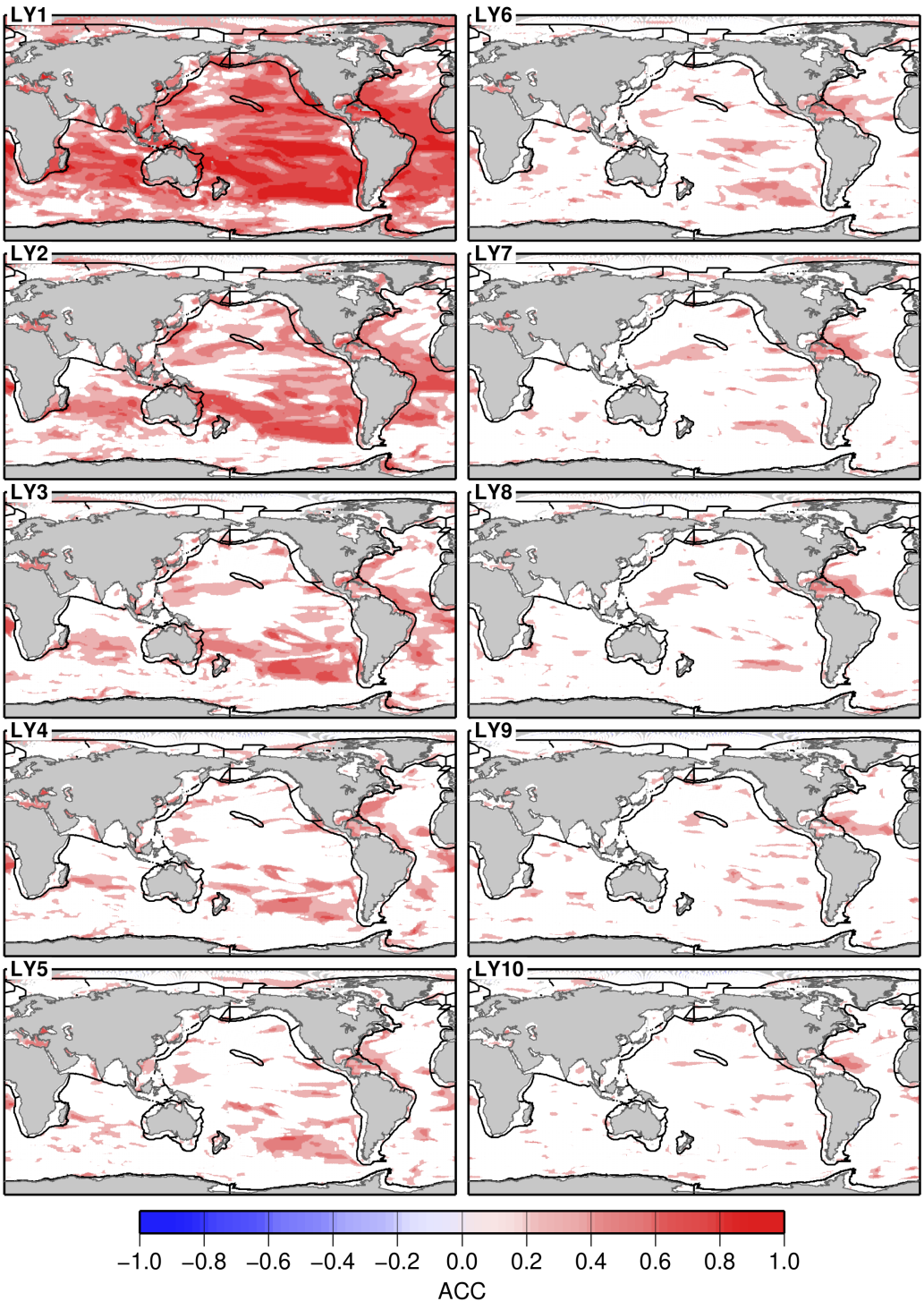

Figure S4. Depth-integrated chlorophyll anomaly correlation coefficients (ACC; potential predictability) between the CESM-DPLE forecasts and the CESM-FOSI reconstruction. Only significant correlations are shown; white areas denote non-significant correlations.

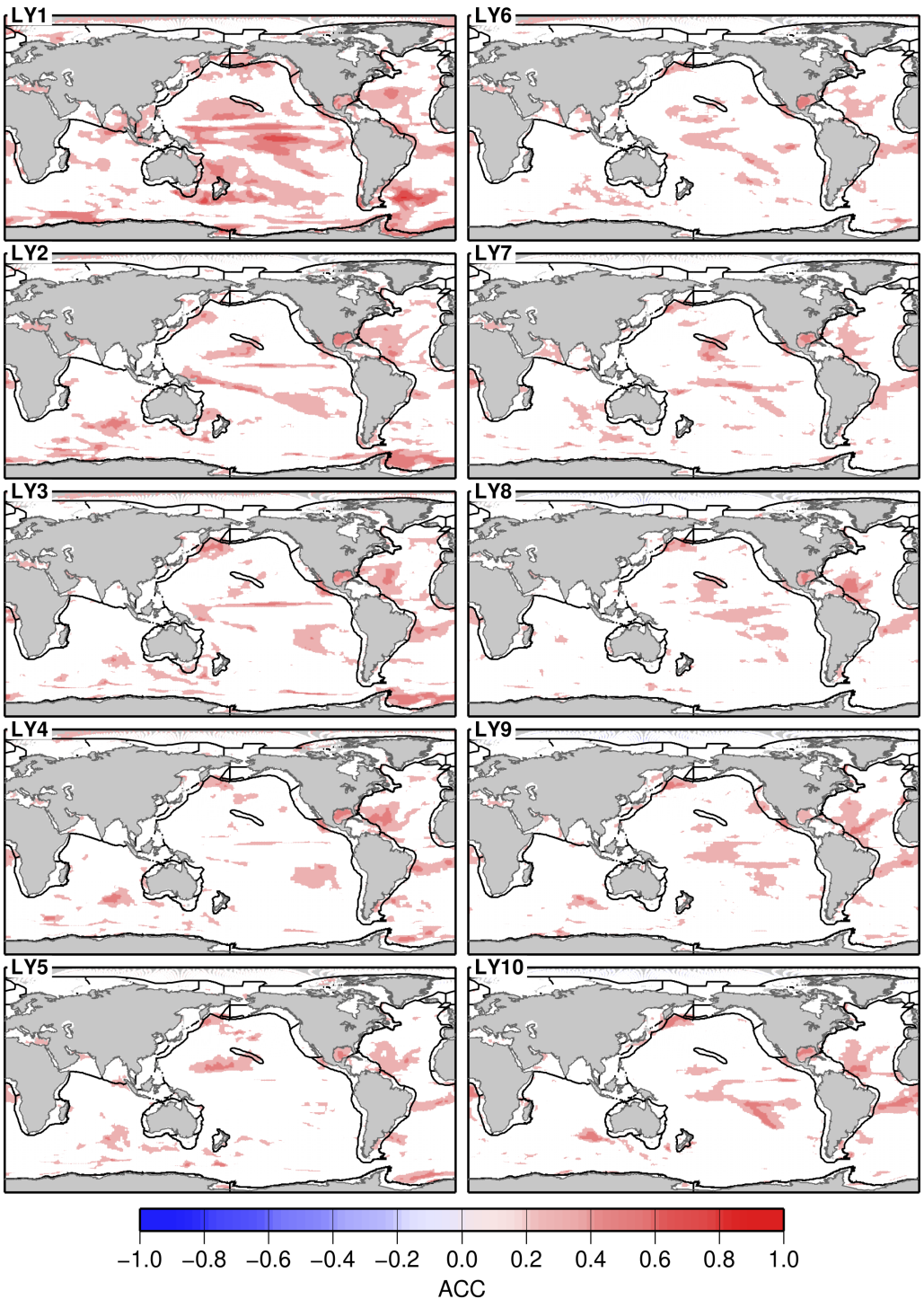

Figure S5. Surface photosynthetically active radiation (PAR) anomaly correlation coefficients (ACC; potential predictability) between the CESM-DPLE forecasts and the CESM-FOSI reconstruction. Only significant correlations are shown; white areas denote non-significant correlations.

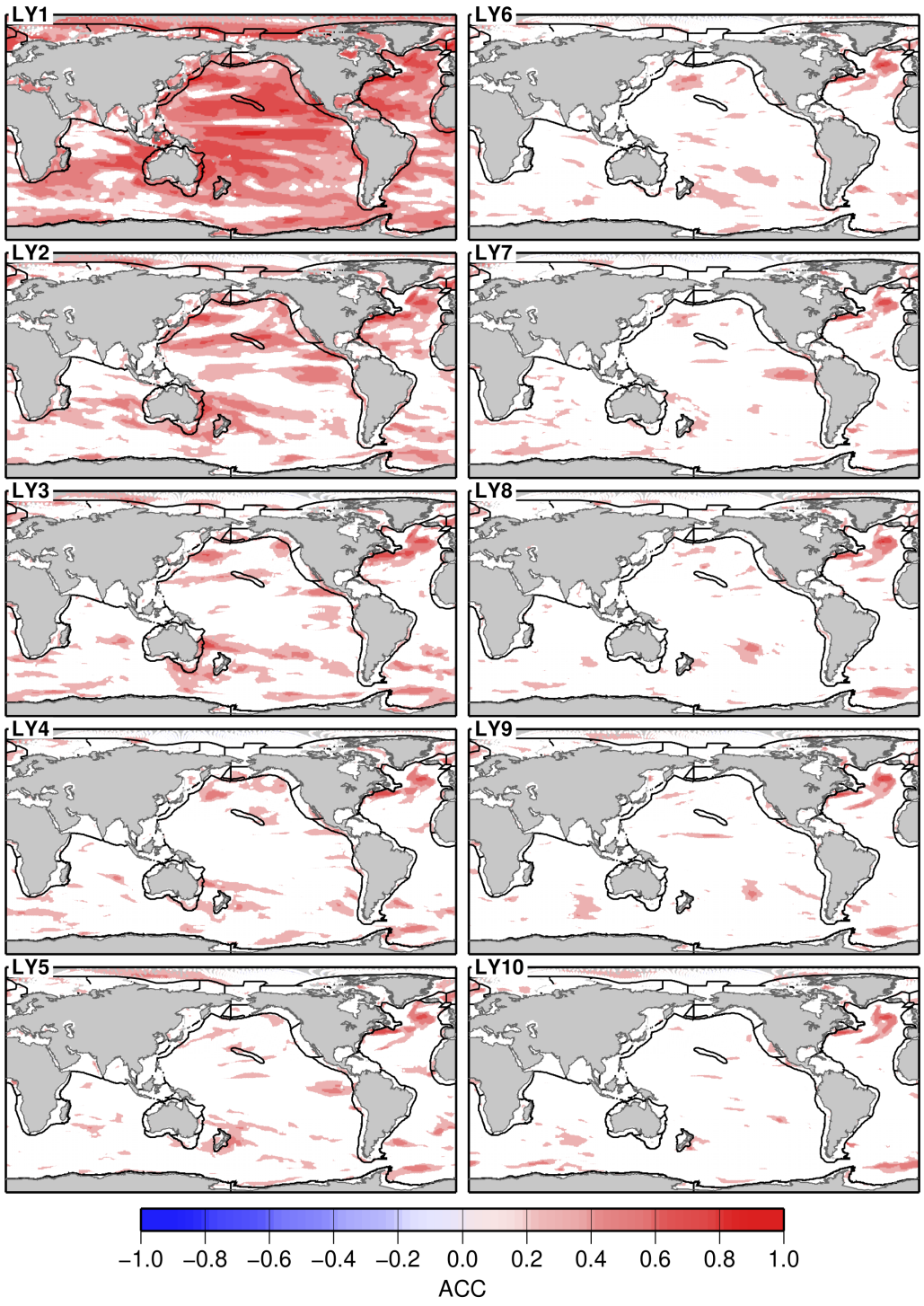

Figure S6. Mixed layer depth anomaly correlation coefficients (ACC; potential predictability) between the CESM-DPLE forecasts and the CESM-FOSI reconstruction. Only significant correlations are shown; white areas denote non-significant correlations.

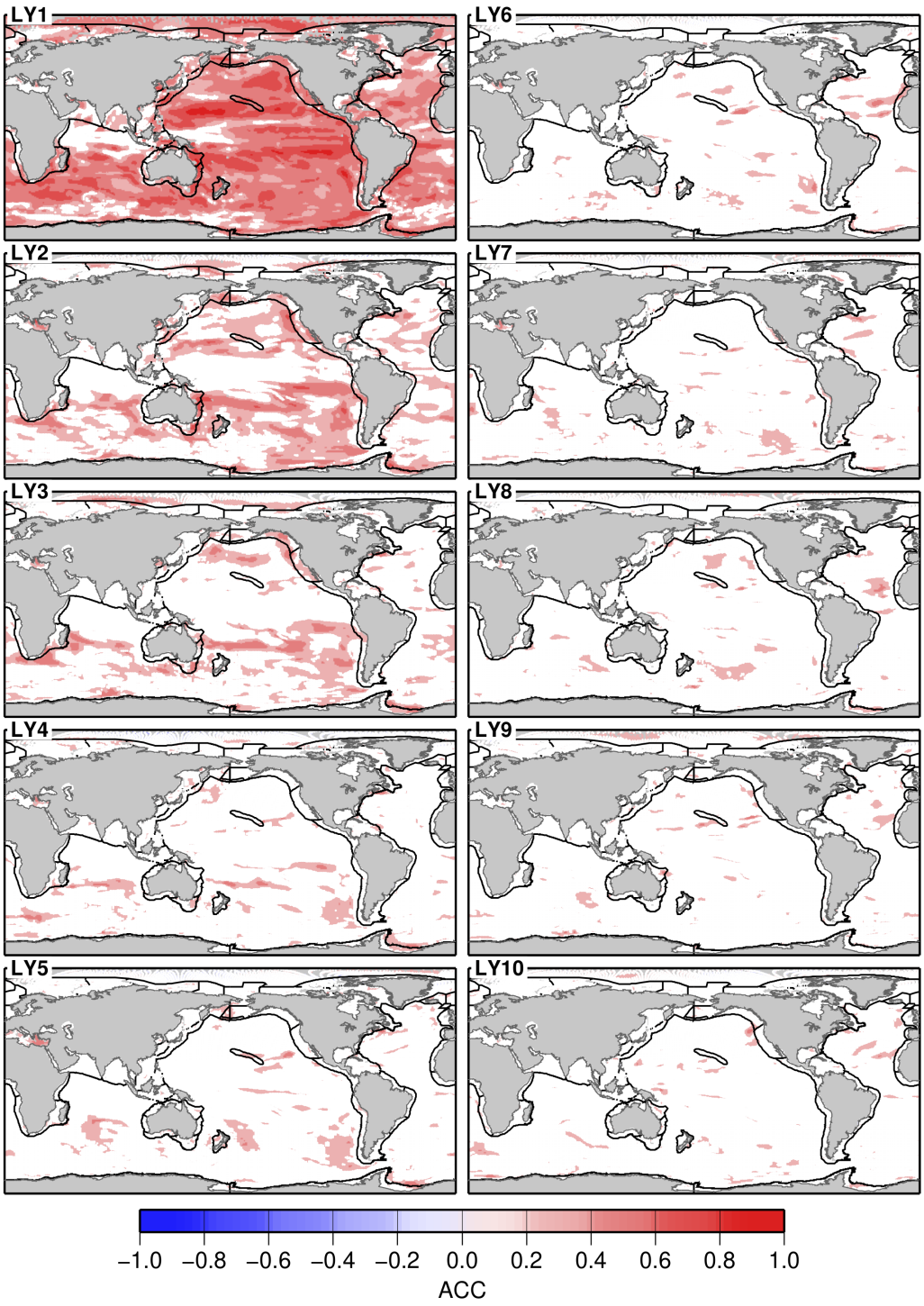

Figure S7. PO_4 physical supply anomaly correlation coefficients (ACC; potential predictability) between the CESM-DPLE forecasts and the CESM-FOSI reconstruction. Only significant correlations are shown; white areas denote non-significant correlations.

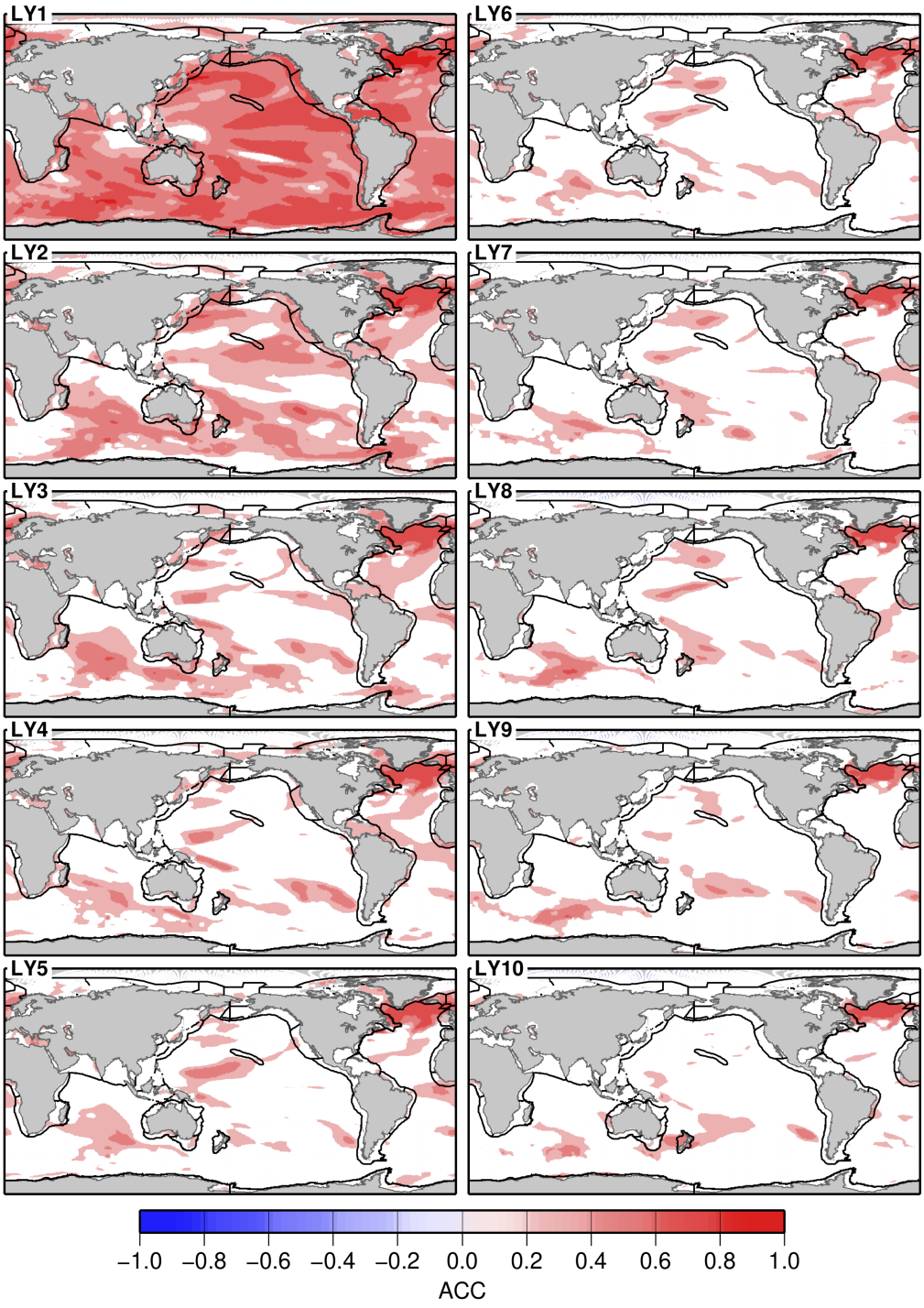

Figure S8. SST anomaly correlation coefficients (ACC; potential predictability) between the CESM-DPLE forecasts and the CESM-FOSI reconstruction. Only significant correlations are shown; white areas denote non-significant correlations.

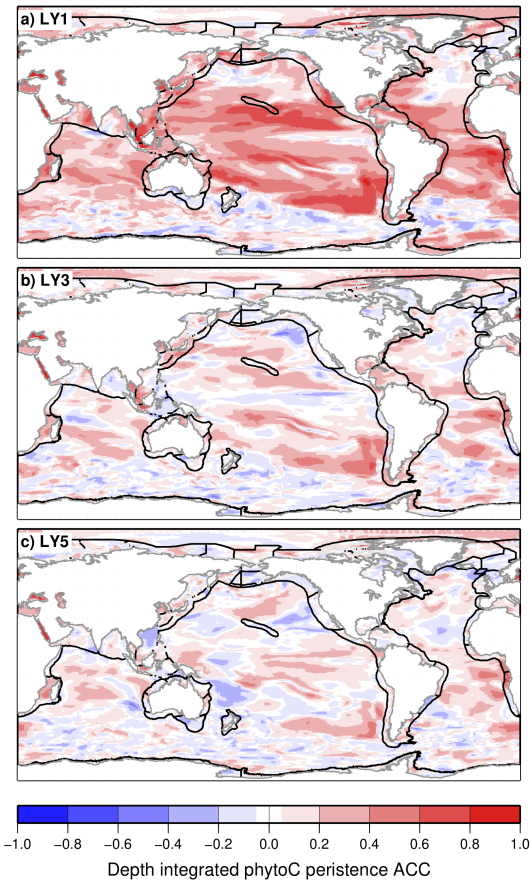

Figure S9. Depth-integrated phytoplankton carbon anomaly correlation coefficients (potential predictability) for a persistence forecast calculated using the CESM-FOSI reconstruction. Only significant correlations are shown; white areas denote non-significant correlations.

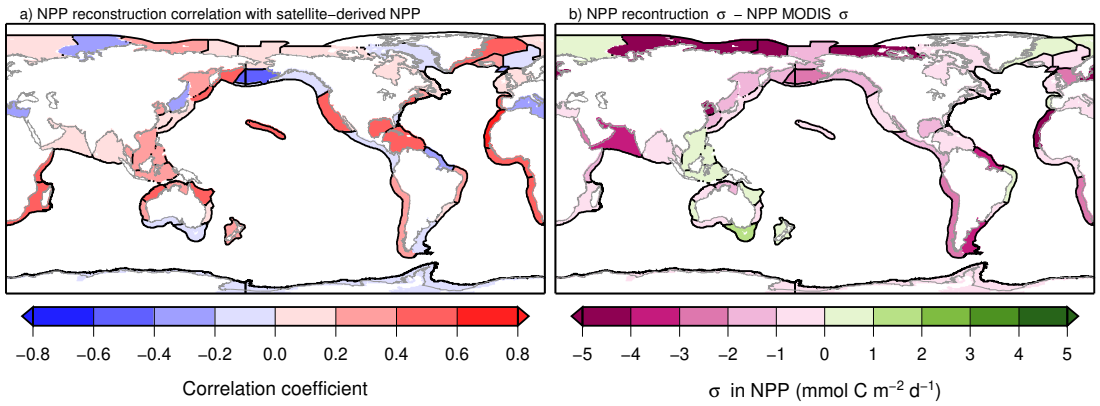

Figure S10. Correlation coefficients between FOSI-hindcast NPP reconstruction and satellite-derived NPP (mean of VGPM, Eppley, and CbPM, see methods) over the period 2003 to 2015 (a) and the difference in standard deviation (σ) between the CESM-FOSI NPP reconstruction and satellite-derived NPP (b) in LMEs. Pink LMEs in panel b represent regions were variability in NPP in the CESM-FOSI reconstruction is less than satellite-derived NPP.

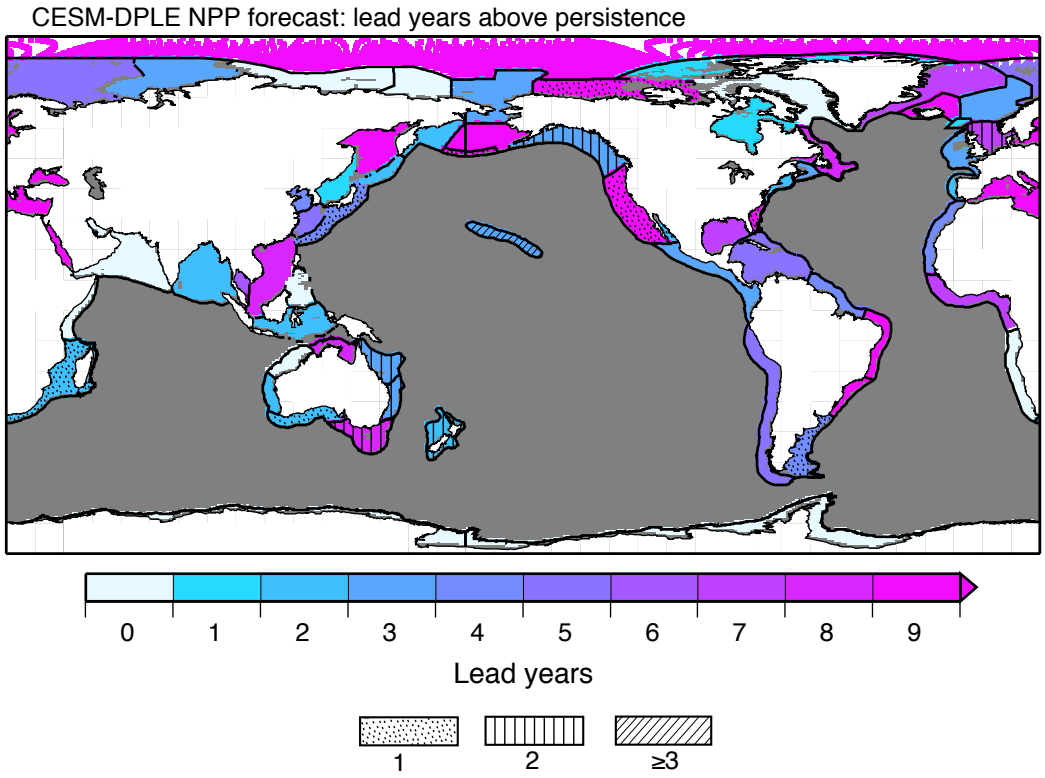

Figure S11. Lead years that the CESM-DPLE forecast has higher predictability than a persistence forecast. Statistically significant improvements over persistence are shown in regions with patterns.